Journal of MATERIALS RESEARCH

Article
DOI: 10.1557/jmr.2019.378

# First report on entire sets of experimentally determined interdiffusion coefficients in quaternary and quinary high-entropy alloys

Vivek Verma[1], Aparna Tripathi[1], Thiruvenkatam Venkateswaran[2], Kaustubh N. Kulkarni[1,a)]

[1]Department of Materials Science and Engineering, Indian Institute of Technology Kanpur, Uttar Pradesh 208016, India
[2]Materials and Mechanical Entity, Vikram Sarabhai Space Centre, Trivandrum, Kerala 695022, India
[a)]Address all correspondence to this author. e-mail: kkaustub@iitk.ac.in

Received: 16 September 2019; accepted: 20 November 2019

**For the first time in the literature, experimental determination of entire sets of exact interdiffusion coefficients in quaternary and quinary alloy systems is reported. Using the method of body-diagonal diffusion couple, a set of nine quaternary interdiffusion coefficients were evaluated in Fe–Ni–Co–Cr and a set of sixteen quinary interdiffusion coefficients were determined in a Fe–Ni–Co–Cr–Mn system, both at approximately equimolar compositions. Regions of uphill interdiffusion and zero flux planes were observed for nickel and cobalt in quinary couples, indicating the existence of strong diffusional interactions in Fe–Ni–Co–Cr–Mn alloys. The strong diffusional interactions were also manifested in the large magnitudes of cross coefficients in both the systems. The existence of strong diffusional interactions in high-entropy alloys (HEAs) as observed through experimentally determined interdiffusion coefficients in this study establishes beyond doubt the fact that cross interdiffusion coefficients cannot be ignored in HEAs.**

## Introduction

The field of high-entropy alloys (HEAs) has captured tremendous attention from researchers over the past two decades due to their potential applications in a variety of sectors, including aerospace, automobile, biomedical, and energy [1, 2, 3, 4, 5]. Although considerable work has been done on HEAs, focusing mostly on exploring their properties, there have been few experimental studies on exploring their fundamental aspects. The most debated topic in HEAs so far is the existence of sluggish diffusion in these alloys [2, 5, 6]. Earlier reports of sluggish diffusion in HEAs were based on the observation of nano-sized precipitates in as-cast $Al_xCoCrCuFeNi$ alloys [7]. These precipitates did not grow or dissolve even after high-temperature annealing, which phenomenon was attributed to the sluggish diffusion in HEAs. Later, in order to understand the diffusion kinetics in HEAs, Tsai et al. [8] performed a series of quasi-binary diffusion couple experiments with Fe–Ni–Co–Cr–Mn alloys. In their work, with the oversimplified assumption of interdiffusion coefficient being equal to intrinsic diffusion coefficient being equal to self-diffusion coefficient, Tsai et al. [8] claimed that the diffusion is sluggish in Fe–Ni–Co–Cr–Mn HEAs. Some studies [9, 10] that followed later also suggested the existence of sluggish diffusion in HEAs. However, Some of the recent articles have reported that diffusion does not necessarily slow down with increasing number of components [6, 11, 12], whereas others have suggested that sluggish diffusion effects exist only for some elements [13, 14] or for some specific compositions [15] and cannot be generalized to all alloys. Some studies have also suggested that sluggish diffusion exists for interdiffusion but not for tracer diffusion [16, 17]. The only direct evidence of sluggishness should come from experimental tracer diffusivity measurements. Vaidya et al. [18, 19] were the first to report experimental tracer diffusivities in Fe–Ni–Co–Cr and Fe–Ni–Co–Cr–Mn HEAs. Based on the comparison of their tracer diffusivity data in HEAs with lower order systems, Vaidya et al. [18, 19] concluded that tracer diffusion does not seem to be slowed down with increasing number of components. This was further confirmed with more radio tracer measurements [20] and with a combination of radiotracer and interdiffusion experiments [21].

Although sluggishness of diffusion is a theoretically important issue, interdiffusion of components is a practically

more significant phenomenon as most of the phase transformations are driven by interdiffusion. Verma et al. [22] have shown, with a set of quinary diffusion couples, that interdiffusion in HEAs can be enhanced or reduced based on diffusional interactions among components and the way their concentration gradients are set up. They estimated the interdiffusion coefficients and diffusional interactions based on Manning's equation [23] by using the experimental tracer diffusion coefficients measured by Vaidya et al. [18, 19]. However, experimental measurement of interdiffusion coefficients in quaternary and quinary systems was still lacking because of the lack of a suitable technique for such measurements. Kulkarni and Chauhan [24] reported average interdiffusion coefficients in a Fe–Ni–Co–Cr system using the Dayananda–Sohn analysis [25]. However, it should be noted that average interdiffusion coefficients, as the name suggests, are only average values of interdiffusion coefficients over a selected range of compositions, and their usage should be limited to only qualitative estimates of diffusional interactions in multicomponent systems. Recently, pseudo-binary [26] and pseudo-ternary [27] diffusion couple techniques have been developed to study interdiffusion in multicomponent systems. The pseudo-binary approach is characterized by variation of concentrations of only two components in an $n$-component diffusion couple. Assuming that there is no uphill diffusion occurring in the diffusion zone of the couple, a pseudo-binary couple can help in determining one out of $(n-1)^2$ interdiffusion coefficients at various compositions developed in the couple. In a pseudo-ternary diffusion couple, three components can develop gradients in their concentrations. If one can design two pseudo-ternary couples with a common composition developed within their diffusion zone, one can estimate four out of $(n-1)^2$ interdiffusion coefficients at the common composition. The absence of uphill diffusion in any of the non-varying components is a necessity for realizing a desired set of pseudo-ternary couples. It should be noted that a quinary system is characterized by sixteen interdiffusion coefficients and a quaternary by nine coefficients. With a pseudo-binary couple, one can only get one main interdiffusion coefficient in the system, whereas with a pseudo-ternary couple, one can get four interdiffusion coefficients. More importantly, both these approaches require that diffusional interactions in the system are negligible so that no uphill interdiffusion regions are generated for non-varying components in the diffusion zones of these couples. Thus, such an approach can only be used when the diffusional interactions are absent or, in other words, when the cross interdiffusion coefficients can be neglected within the diffusion zone. As reported by Verma et al. [22], diffusional interactions in HEAs are expected to be strong, which can only be confirmed based on the knowledge of entire sets of interdiffusion coefficients. An elaborate experimental approach that can estimate a complete set of interdiffusion coefficients in quaternary and higher order systems has been missing so far. Recently, Morral [28] proposed a practically feasible approach to determine interdiffusion coefficients in multicomponent systems using body-diagonal diffusion couples. However, it has not yet been used to evaluate experimental interdiffusion coefficients. The purpose of the present work is to report the first experimental determination of exact sets of quaternary and quinary interdiffusion coefficients, and Morral's newly proposed methodology of body-diagonal couples [28] has been used for this purpose.

## Background and methodology

Interdiffusion in an $n$-component system is described by Onsager's formalism of Fick's law [29], which gives the interdiffusion flux of component $i$, $\tilde{J}_i$ as a linear combination of concentration gradients ($\partial C_j/\partial x$) of all independent components ($j$) as follows:

$$\tilde{J}_i = -\sum_{j=1}^{n-1} \tilde{D}_{ij}^{n} \frac{\partial C_j}{\partial x} \quad , \tag{1}$$

where $\tilde{D}_{ij}^{n}$ are $(n-1)^2$ interdiffusion coefficients, which in turn are functions of compositions. Thus, a ternary system has two independent interdiffusion fluxes, and one needs four interdiffusion coefficients to describe the interdiffusion process at a particular ternary composition. Experimental determination of ternary interdiffusion coefficients has been possible by Kirkaldy's method [30], which requires two independent diffusion couples having at least one common composition in their diffusion zones. This, in other words, means that the diffusion paths of the two couples should intersect at least at one composition. Kirkaldy's method can, in principle, be extended to quaternary and higher order systems. Thus, for determination of nine quaternary interdiffusion coefficients, one would require three independent couples, and for sixteen quinary interdiffusion coefficients, one would require four independent couples with at least one common composition in each respective set of couples. However, it is not practical to predict, for example, for a quaternary system, three diffusion couples with diffusion paths that would intersect at one common composition. Therefore, Kirkaldy's method has been useful for ternary systems but has not yet been applied to quaternary and higher order systems. Recently, Morral [28] proposed a method to select terminal alloy compositions of multicomponent diffusion couples so that Kirkaldy's method can be extended to higher order systems. The method is called body-diagonal diffusion couple method and, as the name suggests, it involves selecting terminal alloy compositions from opposite ends of a diagonal of a hypercube formed in the $(n-1)$

dimensional composition space. Such a couple is characterized by the same difference in the terminal concentrations for all $(n-1)$ independent components. The $n$th (dependent) component makes up for the total of each composition to 100 at.%. This method is explained here for a quaternary system with the help of Fig. 1, which shows a cube formed in the quaternary composition space of three independent concentration variables ($C_1$, $C_2$, and $C_3$).

One has to first decide the terminal composition difference ($\Delta C^0$) and the average composition $\bar{C}$. Setting the origin at the average composition, the eight corners of the cube (representing the desired alloy compositions) can be obtained. In the quaternary example shown in Fig. 1, the eight compositions are $\Delta C^0/2[1,1,1], \Delta C^0/2[\bar{1},\bar{1},\bar{1}], \Delta C^0/2[1,1,\bar{1}], \Delta C^0/2[\bar{1},\bar{1},1]$, $\Delta C^0/2[\bar{1},1,1], \Delta C^0/2[1,\bar{1},\bar{1}], \Delta C^0/2[1,\bar{1},1], \Delta C^0/2[\bar{1},1,\bar{1}]]$ Thus, for a quaternary system, four body-diagonal couples can be obtained for a given set of $\Delta C^0$ and $\bar{C}$. Similarly, for a quinary system, six body-diagonal couples can be set up. Of course, one has to consider two constraints while deciding the couples, viz., avoiding the possibility of the diffusion path crossing out of a single-phase region, in which case we would get a multiphase diffusion zone, and not obtaining negative concentration values, which is unrealistic.

If one selects $\Delta C^0$ to be small, the change in interdiffusion coefficients within the diffusion zone may not be significant. This means that the diffusion path of each of the couples would be symmetric and intersect the body-diagonal at its mid-point. Thus, we can obtain $(n-1)$ diffusion couples whose diffusion paths intersect at one common point $\bar{C}$. Even though the diffusion paths may not intersect exactly at one point, the intersections may lie close to each other so that they can be considered to be at one common composition within the experimental errors.

In the present work, interdiffusion coefficients in quaternary and quinary equimolar compositions were evaluated by using a body-diagonal diffusion couple approach. For the quaternary system, $\Delta C^0 = 10$ and $\bar{c}$= (25, 25, 25, 25), and for the quinary system, $\Delta C^0 = 6$ and $\bar{c}$= (20, 20, 20, 20, 20) were taken. The quaternary and quinary diffusion couples with their designations and the nominal compositions of the terminal alloys used in this study are presented in Table I.

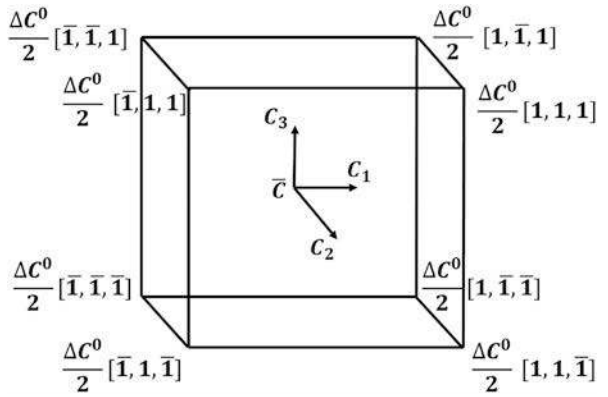


**Figure 1:** Scheme of selection of terminal alloys for body-diagonal diffusion couples in a quaternary system.

**TABLE I:** Nominal compositions of the alloys used for assembling quaternary and quinary diffusion couples.

| Diffusion couple | Terminal alloys | Nominal alloy composition (at.%) | | | | |
|---|---|---|---|---|---|---|
| | | Fe | Ni | Co | Cr | Mn |
| I | E1 | 40 | 20 | 20 | 20 | ... |
| | E2 | 10 | 30 | 30 | 30 | ... |
| H | E3 | 30 | 30 | 20 | 20 | ... |
| | E4 | 20 | 20 | 30 | 30 | ... |
| K | E5 | 20 | 30 | 30 | 20 | ... |
| | E6 | 30 | 20 | 20 | 30 | ... |
| D | Q1 | 32 | 17 | 17 | 17 | 17 |
| | Q2 | 8 | 23 | 23 | 23 | 23 |
| E | Q3 | 20 | 17 | 23 | 23 | 17 |
| | Q4 | 20 | 23 | 17 | 17 | 23 |
| G | Q5 | 14 | 17 | 23 | 23 | 23 |
| | Q6 | 26 | 23 | 17 | 17 | 17 |
| F | Q7 | 14 | 23 | 17 | 23 | 23 |
| | Q8 | 26 | 17 | 23 | 17 | 17 |

## Results and discussion

### Concentration and interdiffusion flux profiles

The concentration profiles for the quaternary diffusion couples H, I, and K are presented in Figs. 2(a), 2(b), and 2(e), respectively. Similarly, the concentration profiles for the four quinary diffusion couples D, E, F, and G are presented in Figs. 3(a), 3(b), 3(e), and 3(f), respectively. The experimental concentration profiles were fitted with the help of the computer program *Multi*DiFlux [31], which fits the profiles with cubic Hermite interpolation polynomials. The profiles are fitted piecewise, and the program also makes sure that the profiles are continuous at the nodes. In order to avoid errors in the interdiffusion fluxes due to scatter in the terminal compositions, the scatter in the experimental concentration data in the terminal regions of the alloys was neglected and the derivatives of the profiles were set to zero in the two terminal ends of each couple. In the concentration profiles shown in Figs. 2 and 3, the experimental data are presented by symbols and the fitted data are presented by solid lines.

The interdiffusion fluxes were determined from the experimental concentration profiles based on the equation proposed by Dayananda and Kim [32]:

$$\tilde{J}_i(x) = \frac{1}{2t}\int_{C_i^-}^{C_i(x)} (x - x_0)\,dC_i \qquad (2)$$

where $t$ is the diffusion annealing time and $x_0$ denotes the position of the Matano plane. In the present work, the molar volumes were assumed constant, in which case the positions of

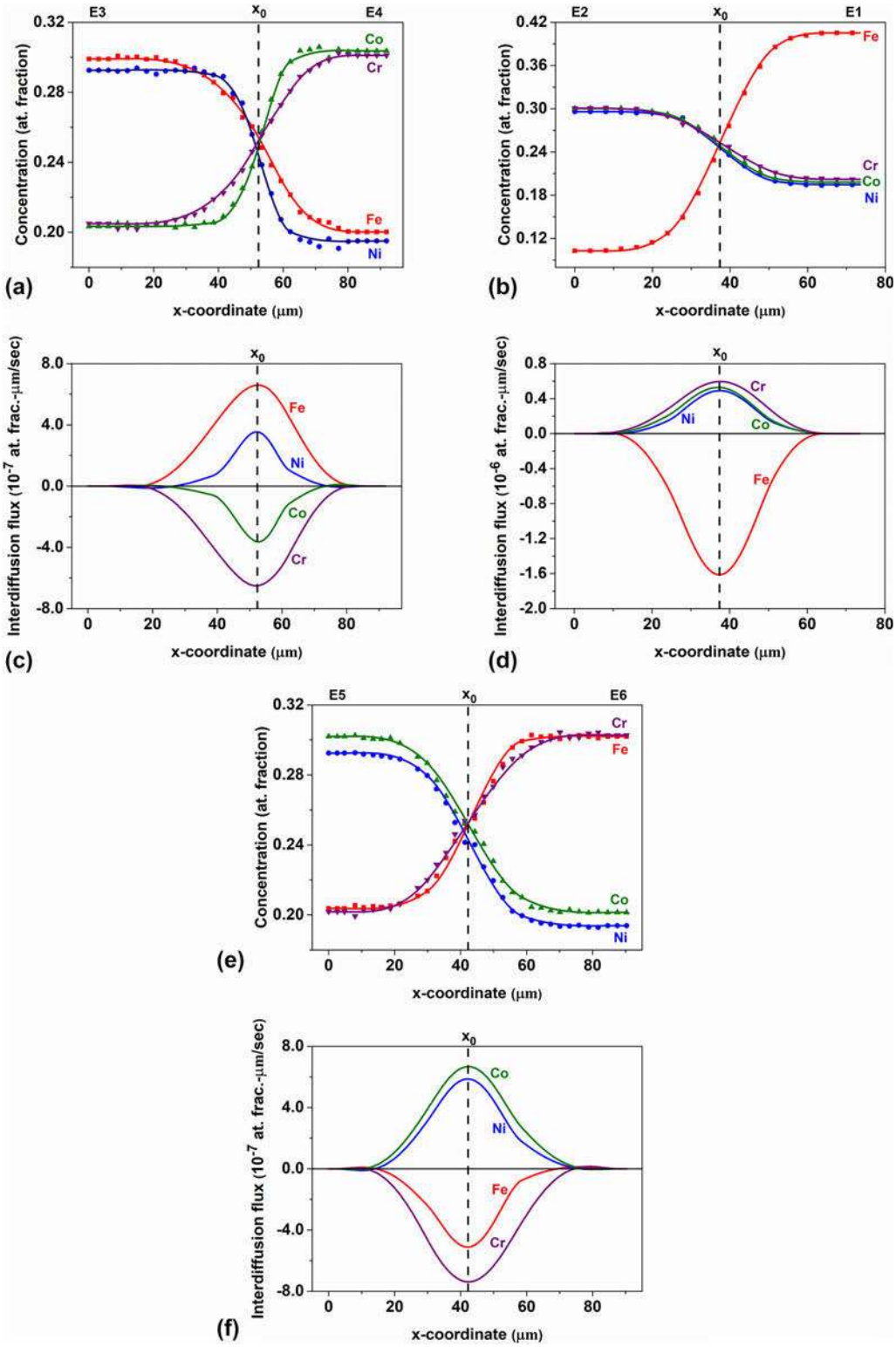


**Figure 2:** Concentration and flux profiles developed in the diffusion zone of quaternary couples H, I, and K annealed at 1000 °C for 100 h (a, c), (b, d), and (e, f), respectively.

the Matano planes for all components should coincide. Location of the Matano plane and determinations of interdiffusion fluxes were also carried out by the *Multi*DiFlux program. The interdiffusion flux profiles for the quaternary couples are presented in Figs. 2(c), 2(d), and 2(f), whereas those for quinary couples are presented in Figs. 3(c), 3(d), 3(g), and 3(h).

For the quaternary diffusion couples, the maximum difference in the position of the Matano planes for all components is less than 1 μm, and for the quinary diffusion couples, it is less than 2.5 μm, which is less than 1.5% of the diffusion depths for all the diffusion couples studied in the present work. This small variation in the position of the Matano plane justifies the assumption of constant molar volume for this study and is not expected to affect much the determination of interdiffusion coefficient values.

## Quaternary interdiffusion

If chromium is treated as a dependent component, the three independent interdiffusion fluxes in the Fe–Ni–Co–Cr system can be expressed, based on Eq. (1), as:

$$\tilde{J}_{\mathrm{Fe}} = -\tilde{D}^{\mathrm{Cr}}_{\mathrm{FeFe}}\frac{\partial C_{\mathrm{Fe}}}{\partial x} - \tilde{D}^{\mathrm{Cr}}_{\mathrm{FeNi}}\frac{\partial C_{\mathrm{Ni}}}{\partial x} - \tilde{D}^{\mathrm{Cr}}_{\mathrm{FeCo}}\frac{\partial C_{\mathrm{Co}}}{\partial x}, \quad (3)$$

$$\tilde{J}_{\mathrm{Ni}} = -\tilde{D}^{\mathrm{Cr}}_{\mathrm{NiFe}}\frac{\partial C_{\mathrm{Fe}}}{\partial x} - \tilde{D}^{\mathrm{Cr}}_{\mathrm{NiNi}}\frac{\partial C_{\mathrm{Ni}}}{\partial x} - \tilde{D}^{\mathrm{Cr}}_{\mathrm{NiCo}}\frac{\partial C_{\mathrm{Co}}}{\partial x}, \quad (4)$$

$$\tilde{J}_{\mathrm{Co}} = -\tilde{D}^{\mathrm{Cr}}_{\mathrm{CoFe}}\frac{\partial C_{\mathrm{Fe}}}{\partial x} - \tilde{D}^{\mathrm{Cr}}_{\mathrm{CoNi}}\frac{\partial C_{\mathrm{Ni}}}{\partial x} - \tilde{D}^{\mathrm{Cr}}_{\mathrm{CoCo}}\frac{\partial C_{\mathrm{Co}}}{\partial x}, \quad (5)$$

If three quaternary diffusion paths intersect at one common composition, we can set up nine independent equations based on Eqs. (3)–(5) and solve them simultaneously for the nine interdiffusion coefficients at the common composition. Diffusion paths for the body-diagonal quaternary diffusion couples H, I, and K are presented in Fig. 4. Diffusion paths for both couples I and K intersect couple H, and the compositions at the two crossover points are within ±0.2 at.%. The crossover composition in at.% is (25.4 ± 0.2Fe, 24.3 ± 0.1Ni, 25 ± 0.2Co, 25.3 ± 0.1Cr), which is also within ±0.8 at.% of the equimolar composition. Quaternary interdiffusion coefficients could be evaluated at the crossover composition by using Kirkaldy's approach, with the assumption that the interdiffusion coefficients do not vary much with a ±0.2 at.% change in the individual concentrations. The quaternary interdiffusion coefficients so evaluated are presented in Table II.

The interdiffusion coefficients at the quaternary equimolar composition of the Fe–Ni–Co–Cr system were also evaluated based on Manning's model [23]. The tracer diffusivity data required for this purpose were taken from those reported by Vaidya et al. [19], and the thermodynamic factors were evaluated by the computational thermodynamic software Thermocalc. The methodology for evaluating multicomponent interdiffusion coefficients based on the knowledge of tracer diffusivities and thermodynamic factors is explained in our earlier publication [22]. The quaternary interdiffusion coefficients calculated based on Manning's model are also reported in Table II. Agreement of the experimental data with the calculated data is excellent.

## Quinary interdiffusion

The four independent interdiffusion fluxes in the Fe–Ni–Co–Cr–Mn system with Cr treated as the dependent component can be expressed, based on Eq. (1), as:

$$\tilde{J}_{\mathrm{Fe}} = -\tilde{D}^{\mathrm{Cr}}_{\mathrm{FeFe}}\frac{\partial C_{\mathrm{Fe}}}{\partial x} - \tilde{D}^{\mathrm{Cr}}_{\mathrm{FeNi}}\frac{\partial C_{\mathrm{Ni}}}{\partial x} - \tilde{D}^{\mathrm{Cr}}_{\mathrm{FeCo}}\frac{\partial C_{\mathrm{Co}}}{\partial x} - \tilde{D}^{\mathrm{Cr}}_{\mathrm{FeMn}}\frac{\partial C_{\mathrm{Mn}}}{\partial x}, \quad (6)$$

$$\tilde{J}_{\mathrm{Ni}} = -\tilde{D}^{\mathrm{Cr}}_{\mathrm{NiFe}}\frac{\partial C_{\mathrm{Fe}}}{\partial x} - \tilde{D}^{\mathrm{Cr}}_{\mathrm{NiNi}}\frac{\partial C_{\mathrm{Ni}}}{\partial x} - \tilde{D}^{\mathrm{Cr}}_{\mathrm{NiCo}}\frac{\partial C_{\mathrm{Co}}}{\partial x} - \tilde{D}^{\mathrm{Cr}}_{\mathrm{NiMn}}\frac{\partial C_{\mathrm{Mn}}}{\partial x}, \quad (7)$$

$$\tilde{J}_{\mathrm{Co}} = -\tilde{D}^{\mathrm{Cr}}_{\mathrm{CoFe}}\frac{\partial C_{\mathrm{Fe}}}{\partial x} - \tilde{D}^{\mathrm{Cr}}_{\mathrm{CoNi}}\frac{\partial C_{\mathrm{Ni}}}{\partial x} - \tilde{D}^{\mathrm{Cr}}_{\mathrm{CoCo}}\frac{\partial C_{Co}}{\partial x} - \tilde{D}^{\mathrm{Cr}}_{\mathrm{CoMn}}\frac{\partial C_{\mathrm{Mn}}}{\partial x}, \quad (8)$$

$$\tilde{J}_{\mathrm{Mn}} = -\tilde{D}^{\mathrm{Cr}}_{\mathrm{MnFe}}\frac{\partial C_{\mathrm{Fe}}}{\partial x} - \tilde{D}^{\mathrm{Cr}}_{\mathrm{MnNi}}\frac{\partial C_{\mathrm{Ni}}}{\partial x} - \tilde{D}^{\mathrm{Cr}}_{\mathrm{MnCo}}\frac{\partial C_{\mathrm{Co}}}{\partial x} - \tilde{D}^{\mathrm{Cr}}_{\mathrm{MnMn}}\frac{\partial C_{\mathrm{Mn}}}{\partial x}. \quad (9)$$

Diffusion paths for the body-diagonal quinary diffusion couples D, E, F, and G are also intersecting within ±0.5 at.%, and the crossover composition can be considered to be in at.% as (19.8 ± 0.4Fe, 19.4 ± 0.1Ni, 19.7 ± 0.5Co, 21.0 ± 0.3Cr, 20.1 ± 0.5Mn). Hence, with the similar assumption of constancy of interdiffusion coefficient within ±0.5 at.% variation in individual concentrations, the sixteen quinary interdiffusion coefficients were determined by Kirkaldy's method, and they are presented in Table III along with those calculated based on Manning's model. Note that the cross-over composition is also within ±1.3 at.% of the equimolar composition. The experimental data agree reasonably well with the calculated data.

## Validity and utility of multicomponent interdiffusion data in HEAs

It should be noted that in employing the body-diagonal diffusion couple approach, it is assumed that the interdiffusion coefficients do not vary much over the small composition range of the two terminal alloys. Constancy of interdiffusion coefficients also implies that the diffusion profiles should be symmetric and the average of the two terminal alloy compositions should overlap with the composition at the Matano plane. Table IV presents the comparison of the mean compositions of the two terminal alloys with the Matano plane composition for all the quaternary and quinary couples studied, and a very good agreement has been found between the two values for all couples. Moreover, the crossover compositions are very close to equiatomic compositions (±0.8 at.% for quaternary and ±1.3 at.% for quinary), and hence, the measured set of interdiffusion coefficients can also be taken as belonging to the equiatomic compositions within the experimental uncertainties.

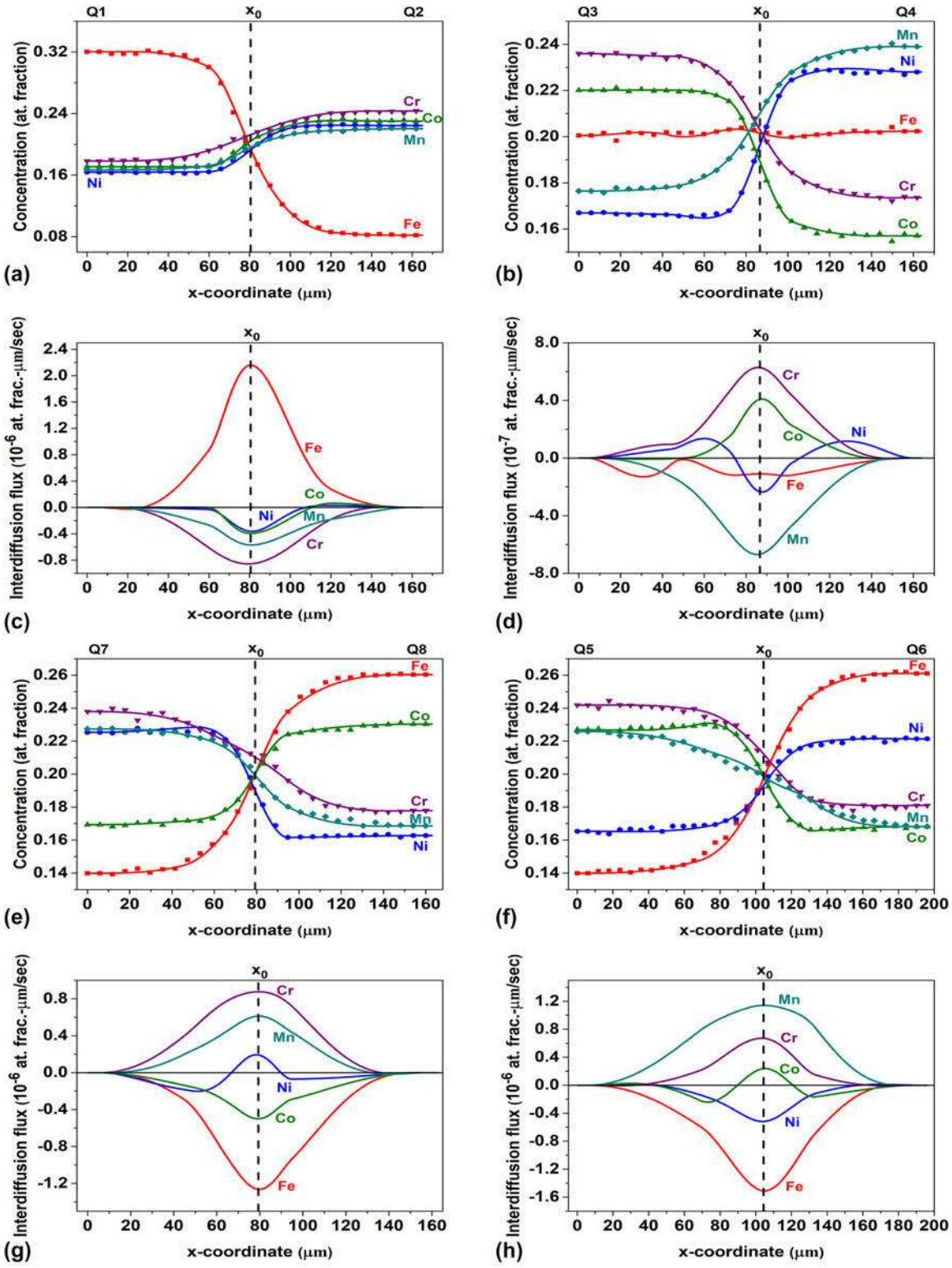


**Figure 3:** Concentration and flux profiles developed in the diffusion zone of quinary couples D, E, F, and G annealed at 1000 °C for 100 h (a, c), (b, d), (e, g), and (f, h), respectively.

For simulation of composition profiles in any process, it is desired to have smooth data of multicomponent interdiffusion coefficients as functions of compositions and temperature. For obtaining such interdiffusivity–composition–temperature relations, CALPHAD approach has been proposed for mobility parameter optimization [33], and some databases are even

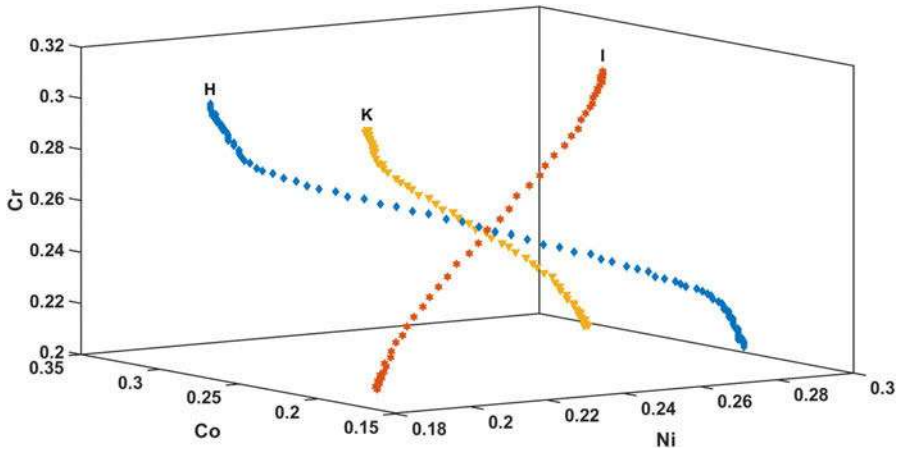


**Figure 4:** Diffusion paths for the body-diagonal quaternary diffusion couples H, I, and K.

**TABLE II:** Quaternary interdiffusion coefficients evaluated in equimolar FeNiCoCr HEA at 1000 °C, with chromium being treated as a dependent component. Interdiffusivities are reported in $10^{-16}$ $m^2/s$.

| Interdiffusivity | $\tilde{D}^{Cr}_{FeFe}$ | $\tilde{D}^{Cr}_{FeNi}$ | $\tilde{D}^{Cr}_{FeCo}$ | $\tilde{D}^{Cr}_{NiFe}$ | $\tilde{D}^{Cr}_{NiNi}$ | $\tilde{D}^{Cr}_{NiCo}$ | $\tilde{D}^{Cr}_{CoFe}$ | $\tilde{D}^{Cr}_{CoNi}$ | $\tilde{D}_{CoCo}$ |
|---|---|---|---|---|---|---|---|---|---|
| Experimental | 1.4 | 0.2 | −0.1 | 0.3 | 1.2 | 0.8 | 0.4 | 0.8 | 1.6 |
| Estimated by Manning's model | 1.9 | 0.3 | 0.2 | 0.2 | 1.2 | 0.9 | 0.2 | 0.9 | 1.6 |

being developed in HEA systems [11] using this approach. Availability of experimental interdiffusion data in multicomponent systems would be necessary for validating the interdiffusion coefficients determined with such databases. In light of significant diffusional interactions, the entire sets of experimental interdiffusion coefficients should be taken into account for optimizing and validating the diffusion databases being developed in various multicomponent systems. As clearly illustrated in the present study, the body-diagonal diffusion couple approach can be used to experimentally determine entire sets of interdiffusion coefficients in quaternary and higher order systems at various discreet compositions and temperatures.

## Significance of diffusional interactions in HEAs

Interdiffusion analysis of the quinary Fe–Ni–Co–Cr–Mn couples reveals the presence of significant diffusional interactions determined in terms of concentration profiles, interdiffusion fluxes, and interdiffusion coefficients. As can be seen from Table III, several cross coefficients are about the same order of magnitude as the respective main coefficients. Especially noteworthy are interactions between nickel and manganese, between iron and nickel, between iron and cobalt, and between cobalt and nickel. The large positive value of $\tilde{D}^{Cr}_{FeNi}$ indicates that the interdiffusion flux of iron is enhanced down the concentration gradient of nickel and reduced up the gradient. The cross coefficient $\tilde{D}^{Cr}_{NiMn}$ is negative and more than half in magnitude than the main coefficient $\tilde{D}^{Cr}_{NiNi}$. This indicates that the interdiffusion flux of nickel is enhanced up the concentration gradient of manganese and reduced down the gradient. Similarly, the positive value of $\tilde{D}^{Cr}_{CoNi}$ indicates that the interdiffusion flux of cobalt is enhanced down the gradient of nickel and reduced up the gradient. The strong interactions are also visible in the observed concentration profiles. Nickel shows prominent maximum and minimum on two of the quinary couples, viz., couple E and couple F, as seen from Figs. 3(b) and 3(e), respectively. Correspondingly, two zero flux planes are exhibited by nickel in each of the two couples. Similarly, cobalt exhibits two zero flux planes in couple G, as seen from Fig. 3(h). The appearance of zero flux planes and regions of uphill interdiffusion corroborates the presence of strong diffusional interactions in the Fe–Ni–Co–Cr–Mn HEA.

The strong diffusional interaction observed between nickel and manganese is consistent with the prediction and observations of Verma et al. [22]. In their study, Verma et al. [22] predicted that the Ni–Mn pair should be exhibiting strong negative diffusional interactions in Fe–Ni–Co–Cr–Mn quinary HEA alloys, and based on this, they designed the diffusion couples, which exhibited enhancement and reduction of interdiffusion in this system consistent with the predictions of the diffusional interactions.

It can be seen from the experimental interdiffusion coefficients reported for quaternary Fe–Ni–Co–Cr HEA in Table II that all the cross coefficients, except for $\tilde{D}^{Cr}_{FeCo}$, are positive. A comparison between the main interdiffusion

**TABLE III:** Quinary interdiffusion coefficients evaluated through the body-diagonal diffusion couple approach in equimolar FeNiCoCrMn HEA at 1000 °C, with chromium being treated as a dependent component. Interdiffusivities are reported in $10^{-16}$ $m^2/s$.

| Interdiffusivity | $\tilde{D}^{Cr}_{FeFe}$ | $\tilde{D}^{Cr}_{FeNi}$ | $\tilde{D}^{Cr}_{FeCo}$ | $\tilde{D}^{Cr}_{FeMn}$ | $\tilde{D}^{Cr}_{NiFe}$ | $\tilde{D}^{Cr}_{NiNi}$ | $\tilde{D}^{Cr}_{NiCo}$ | $\tilde{D}^{Cr}_{NiMn}$ |
|---|---|---|---|---|---|---|---|---|
| Experimental | 5.5 | 4.1 | 2.8 | −1.0 | 0.6 | 3.3 | 1.4 | −1.9 |
| Obtained by Manning's model | 3.2 | 1.5 | 1.1 | −1.8 | 0.5 | 4.0 | 1.9 | −2.8 |
| Interdiffusivity | $\tilde{D}^{Cr}_{CoFe}$ | $\tilde{D}^{Cr}_{CoNi}$ | $\tilde{D}^{Cr}_{CoCo}$ | $\tilde{D}^{Cr}_{CoMn}$ | $\tilde{D}^{Cr}_{MnFe}$ | $\tilde{D}^{Cr}_{MnNi}$ | $\tilde{D}^{Cr}_{MnCo}$ | $\tilde{D}^{Cr}_{MnMn}$ |
| Experimental | 0.8 | 1.5 | 3.2 | −0.1 | −0.3 | −3.3 | −0.5 | 9.1 |
| Obtained by Manning's model | 0.5 | 2.1 | 3.2 | −2.2 | −1.0 | −5.1 | −3.3 | 12.1 |

**TABLE IV:** Comparison of the mean composition of the two terminal alloys with the Matano plane composition for all the quaternary and quinary couples studied.

| | | | Concentrations (at.%) | | | | |
|---|---|---|---|---|---|---|---|
| System | Couple | Composition type | Fe | Ni | Co | Cr | Mn |
| Quaternary | H | Average of terminal alloys | 24.9 | 24.4 | 25.4 | 25.3 | ... |
| | | At Matano plane | 25.4 | 24.4 | 24.9 | 25.3 | ... |
| | I | Average of terminal alloys | 25.4 | 24.5 | 24.9 | 25.2 | ... |
| | | At Matano plane | 25.3 | 24.6 | 24.8 | 25.3 | ... |
| | K | Average of terminal alloys | 25.3 | 24.3 | 25.2 | 25.2 | ... |
| | | At Matano plane | 25.2 | 24.3 | 25.2 | 25.3 | ... |
| Quinary | D | Average of terminal alloys | 20.1 | 19.4 | 20.0 | 21.1 | 19.4 |
| | | At Matano plane | 19.4 | 19.3 | 20.4 | 21.3 | 19.6 |
| | E | Average of terminal alloys | 20.1 | 19.7 | 18.9 | 20.5 | 20.8 |
| | | At Matano plane | 20.2 | 19.6 | 18.9 | 20.3 | 21.0 |
| | F | Average of terminal alloys | 20.0 | 19.4 | 20.0 | 20.8 | 19.8 |
| | | At Matano plane | 20.0 | 19.0 | 20.0 | 21.0 | 20.0 |
| | G | Average of terminal alloys | 20.1 | 19.3 | 19.8 | 21.1 | 19.7 |
| | | At Matano plane | 19.7 | 19.3 | 19.9 | 21.2 | 19.9 |

coefficients ($\tilde{D}^{Cr}_{FeFe}, \tilde{D}^{Cr}_{NiNi}$ and $\tilde{D}^{Cr}_{CoCo}$) for quaternary Fe–Ni–Co–Cr and quinary Fe–Ni–Co–Cr–Mn systems from Tables I and II indicates that their values for the quinary system are about two to four times those of the quaternary system. Some reports [16, 17] have suggested that interdiffusion becomes more sluggish with the increasing number of components. However, the present experimental study suggests that the main interdiffusion coefficients are higher in the quinary system than in the quaternary system. It should also be noted, from Eq. (1), that the interdiffusion flux of a component can be reduced or enhanced by diffusional interactions, i.e., the sign and magnitude of cross interdiffusion coefficient as well as relative directions of concentration gradients. This has been discussed and illustrated in our earlier work [22] with specially designed diffusion couples in the Fe–Ni–Co–Cr–Mn system.

The magnitudes of cross interdiffusion coefficients in the quaternary Fe–Ni–Co–Cr system (Table II) are about an order of magnitude smaller than those in quinary Fe–Ni–Co–Cr–Mn. Although the diffusional interactions in the quaternary Fe–Ni–Co–Cr system are not as strong as those in the quinary Fe–Ni–Co–Cr–Mn system, they are still not insignificant. The strongest diffusional interaction in this quaternary system is seen to be between Ni and Co, which is evident from the cross coefficient $\tilde{D}^{Cr}_{NiCo}$, which is about 67% in magnitude with respect to its main coefficient $\tilde{D}^{Cr}_{NiNi}$. The positive value of $\tilde{D}^{Cr}_{NiCo}$ in the quaternary Fe–Ni–Co–Cr system indicates that the interdiffusion flux of nickel is enhanced up the gradient of cobalt in this system. Most of the recent reports on diffusion in HEAs have either completely ignored or underestimated the significance of cross interdiffusion coefficients in these systems. The existence of strong diffusional interactions in HEAs, as observed through the experimentally determined interdiffusion coefficients in this study, establishes beyond doubt the fact that cross coefficients cannot be ignored in HEAs.

## Summary and conclusions

The present study is the first report in the literature on experimental determination of entire and exact sets of quaternary and quinary interdiffusion coefficients. The novel approach of body-diagonal diffusion couples [28] has been successfully applied for the determination of multicomponent interdiffusion coefficients in Fe–Ni–Co–Cr and Fe–Ni–Co–Cr–Mn equimolar alloys, which are commonly referred to as HEAs. This report also corroborates the earlier findings from our group that diffusional interactions are significant in HEAs. The Fe–Ni–Co–Cr–Mn HEA is characterized by strong positive interactions of nickel with iron, positive interactions of nickel with cobalt, and a strong negative interaction of manganese with nickel, which was evident in the positive values of $\tilde{D}^{Cr}_{FeNi}$ and $\tilde{D}^{Cr}_{CoNi}$ and negative value of $\tilde{D}^{Cr}_{NiMn}$, respectively. The presence of strong diffusional interactions in this system was also manifested in the form of maxima and minima on concentration profiles and zero flux planes of nickel and cobalt in some of the couples. The diffusional interactions in the Fe–Ni–Co–Cr equimolar alloy were observed to be not as strong as in the quinary Fe–Ni–Co–Cr–Mn equimolar alloy, yet they are not insignificant.

The existence of strong diffusional interactions in HEAs, as observed through the experimentally determined interdiffusion coefficients in this study, establishes beyond doubt the fact that cross coefficients cannot be ignored in HEAs. This is especially critical because most of the recent reports on diffusion in HEAs have either completely ignored or underestimated the significance of cross interdiffusion coefficients in these systems.

## Experimental methodology

Pure iron granules (purity 99.98%), nickel shots (purity 99.95%), cobalt pieces (purity 99.9%), chromium pieces (purity 99.995%), and manganese pieces (purity 99.95%) supplied by Alfa Aesar, USA, were used as raw materials. Pure materials were weighed in right proportions to make the alloys of desired compositions. Alloys were prepared in a vacuum arc melting furnace in an argon atmosphere. Alloys prepared were in the form of buttons, which then were vacuum sealed in a quartz ampoule for homogenization. Before sealing the ampoule, it was repeatedly evacuated and purged with argon thrice to a pressure of about $10^{-5}$ torr, and final sealing was done with an argon atmosphere inside the ampoule. These sealed buttons were homogenized at 1100 °C for 4 days in a three-zone MTI OTF-1600× tube furnace. Buttons were cut using a low-speed saw; metallographically polished by using emery papers in a sequence of 800, 1000, 1500, and 2000; and then cloth-polished by using diamond paste of 1 μm, followed by 0.05 μm colloidal silica to check for homogenization of the alloys. Terminal alloy blocks of approximate dimensions of 5 mm × 5 mm × 3 mm were cut from the homogenized alloys by using a low-speed saw, keeping in mind that both the surfaces of the terminal alloys should be parallel, which helps in proper bonding of the couple. Then, the alloys were metallographically polished through 0.05 μm colloidal silica. Polished blocks were cleaned ultrasonically in methanol and dried with a hot air drier. Then, the two halves were clamped together in a special jig made of stainless steel discs. Molybdenum foil was used as a spacer between the terminal alloys and the stainless steel discs. The diffusion assembly so formed was sealed in a quartz ampoule with the same procedure as described earlier in this section. The sealed diffusion assemblies were diffusion annealed at a temperature of 1000 °C for 100 h. For better control of temperature for diffusion annealing, the MTI TF-1200× three-zone split tube furnace was used, in which the temperature uniformity was measured as ±1 °C.

After completion of diffusion annealing, diffusion couples were quenched in water. The annealed diffusion couples were sectioned perpendicular to the direction of diffusion by using a low-speed saw. The sectioned surfaces were polished with the same metallographic process as described above for further observations and composition analysis. Point-by-point analyses were conducted to measure the concentration profiles developed in the diffusion zone by using a JEOL JXA-8230 electron probe micro-analyzer (EPMA). Pure elemental standards were used with a probe condition of 25 kV accelerating voltage and 20 nA probe current. $K_\alpha$ X-ray intensities of each element, corrected with ZAF corrections, were used for the measurements.

## Acknowledgments

This work was supported by the Vikram Sarabhai Space Center (VSSC), Thiruvananthapuram, through the Space Technology Cell at IIT Kanpur [STC/MET/2017181]. The authors express their acknowledgment to the Advanced Center for Material Science (ACMS), IIT Kanpur, for providing EPMA facility used in the present investigations. The authors are grateful to Sandvik Asia Pvt. Ltd., Pune, for facilitating the arc melting of a few alloys used in this work.

## References

1. **J.W. Yeh, S.K. Chen, S.J. Lin, J.Y. Gan, T.S. Chin, T.T. Shun, C.H. Tsau, and S.Y. Chang**: Nanostructured high-entropy alloys with multiple principal elements: Novel alloy design concepts and outcomes. *Adv. Eng. Mater.* **6**, 299 (2004).
2. **D.B. Miracle, J.D. Miller, O.N. Senkov, C. Woodward, M.D. Uchic, and J. Tiley**: Exploration and development of high entropy alloys for structural applications. *Entropy* **16**, 494 (2014).
3. **M.H. Tsai and J.W. Yeh**: High-entropy alloys: A critical review. *Mater. Res. Lett.* **2**, 107 (2014).
4. **A. Kumar and M. Gupta**: An insight into evolution of light weight high entropy alloys: A review. *Metals* **6**, 199 (2016).
5. **D.B. Miracle and O.N. Senkov**: A critical review of high entropy alloys and related concepts. *Acta Mater.* **122**, 448 (2017).
6. **S.V. Divinski, A.V. Pokoev, N. Esakkiraja, and A. Paul**: A mystery of "sluggish diffusion" in high-entropy alloys: The truth or a myth? *Mater. Res. Lett.* **17**, 69 (2018).
7. **C.J. Tong, Y.L. Chen, S.K. Chen, J.W. Yeh, T.T. Shun, C.H. Tsau, S.J. Lin, and S.Y. Chang**: Microstructure characterization of $Al_x$CoCrCuFeNi high-entropy alloy system with multiprincipal elements. *Metall. Mater. Trans. A* **36**, 881 (2005).
8. **K.Y. Tsai, M.H. Tsai, and J.W. Yeh**: Sluggish diffusion in Co–Cr–Fe–Mn–Ni high-entropy alloys. *Acta Mater.* **61**, 4887 (2013).
9. **J. Dabrowa, W. Kucza, G. Cieslak, T. Kulik, M. Danielewski, and J-W. Yeh**: Interdiffusion in the FCC-structured Al–Co–Cr–Fe–Ni high entropy alloys: Experimental studies and numerical simulations. *J. Alloys Compd.* **674**, 455 (2016).

10. **D.L. Beke and G. Erdelyi**: On the diffusion in high-entropy alloys. *Mater. Lett.* **164**, 111 (2016).
11. **C. Zhang, F. Zhang, K. Jin, H. Bei, S. Chen, W. Cao, J. Zhu, and D. Lv**: Understanding of the elemental diffusion behaviour in concentrated solid solution alloys. *J. Phase Equilibria Diffusion* **38**, 434 (2017).
12. **M. Vaidya, G.M. Muralikrishna, S.V. Divinksi, and B.S. Murty**: Experimental assessment of the thermodynamic factor for diffusion in CoCrFeNi and CoCrFeMnNi high entropy alloys. *Scr. Mater.* **157**, 81 (2018).
13. **Q. Li, W. Chen, J. Zhong, L. Zhang, Q. Chen, and Z-K. Liu**: On sluggish diffusion in FCC Al–Co–Cr–Fe–Ni high entropy alloys: An experimental and numerical study. *Metals* **8**, 16 (2018).
14. **S. Chen, Q. Li, J. Zhong, F. Xing, and L. Zhang**: On diffusion behaviors in face centered cubic phase of Al–Co–Cr–Fe–Ni–Ti high entropy superalloys. *J. Alloys Compd.* **791**, 255 (2019).
15. **J. Dabrowa, M. Zajusz, W. Kucza, G. Cieslak, K. Berent, T. Czeppe, T. Kulik, and M. Danielewski**: Demystifying the sluggish diffusion effect in high entropy alloys. *J. Alloys Compd.* **783**, 193 (2019).
16. **W. Chen and L. Zhang**: High-throughput determination of interdiffusion coefficients for Co–Cr–Fe–Mn–Ni high entropy alloys. *J. Phase Equilibria Diffusion* **38**, 457 (2017).
17. **R. Wang, W. Chen, J. Zhong, and L. Zhang**: Experimental and numerical studies on the sluggish diffusion in face centred cubic Co–Cr–Cu–Fe–Ni high entropy alloys. *J. Mater. Sci. Technol.* **34**, 1791 (2018).
18. **M. Vaidya, S. Trubel, B.S. Murty, G. Wilde, and S.V. Divinski**: Ni tracer diffusion in CoCrFeNi and CoCrFeMnNi high entropy alloys. *J. Alloys Compd.* **688**, 994 (2016).
19. **M. Vaidya, K.G. Pradeep, B.S. Murty, G. Wilde, and S.V. Divinski**: Bulk tracer diffusion in CoCrFeNi and CoCrFeMnNi high entropy alloys. *Acta Mater.* **146**, 211 (2018).
20. **D. Gaertner, J. Kottke, G. Wilde, S.V. Divinski, and Y. Chumlyaskov**: Tracer diffusion in single crystalline COCrFeNi and CoCrFeMnNi high entropy alloys. *J. Mater. Res.* **33**, 3183 (2018).
21. **D. Gaertner, K. Abrahams, J. Kottke, V.A. Esin, I. Steinbach, G. Wilde, and S.V. Divinski**: Concentration-dependent atomic mobilities in FCC CoCrFeMnNi high entropy alloys. *Acta Mater.* **166**, 357 (2019).
22. **V. Verma, A. Tripathi, and K.N. Kulkarni**: On interdiffusion in FeNiCoCrMn high entropy alloy. *J. Phase Equilibria Diffusion* **38**, 445 (2017).
23. **J.R. Manning**: Cross terms in the thermodynamic diffusion equations for multicomponent alloys. *Metall. Trans. B* **1**, 499 (1970).
24. **K. Kulkarni and G.P.S. Chauhan**: Investigations of quaternary interdiffusion in a constituent system of high entropy alloys. *AIP Adv.* **5**, 097162 (2015).
25. **M.A. Dayananda and Y.H. Sohn**: A new analysis for the determination of ternary interdiffusion coefficients from a single diffusion couple. *Metall. Mater. Trans. A* **30**, 535 (1999).
26. **A. Paul**: A pseudobinary approach to study interdiffusion and the Kirkendall effect in multicomponent systems. *Philos. Mag.* **93**, 2297 (2013).
27. **N. Esakkiraja and A. Paul**: A novel concept of pseudo ternary diffusion couple for the estimation of diffusion coefficients in multicomponent systems. *Scr. Mater.* **147**, 79 (2018).
28. **J.E. Morral**: Body-diagonal diffusion couples for high entropy alloys. *J. Phase Equilibria Diffusion* **39**, 51 (2018).
29. **L. Onsager**: Theories and problems of liquid diffusion. *Ann. N. Y. Acad. Sci.* **46**, 241 (1945).
30. **J.S. Kirkaldy**: Diffusion in multicomponent metallic systems. *Can. J. Phys.* **35**, 435 (1957).
31. **K.M. Day, L.R. Ram-Mohan, and M.A. Dayananda**: Determination and assessment of ternary interdiffusion coefficients from individual diffusion couples. *J. Phase Equilib. Diffus.* **26**, 579 (2005).
32. **M.A. Dayananda and C.W. Kim**: Zero-flux planes and flux reversals in Cu–Ni–Z diffusion couples. *Metall. Trans. A* **10**, 1333 (1979).
33. **J.O. Andersson and J. Agren**: Models for numerical treatment of multicomponent diffusion in simple phases. *J. Appl. Phys.* **72**, 1350 (1992).